Kramers-Kronig dispersive analysis and optical properties in the infrared, and revised vibrational behavior of orthorhombic $Na_2[Fe(CN)_5NO]\cdot 2H_2O$

Oscar E. Piro
Departamento de Física, Facultad de Ciencias Exactas, Universidad Nacional de La Plata, Calle 115 y 49, Casilla de Correo 67, 1900 La Plata, República Argentina

E. E. Castellano
Instituto de Física e Química de São Carlos, Universidade de São Paulo, Caixa Postal 369, 13 560 São Carlos, Estado de São Paulo, Brazil

J. A. Güida and P. J. Aymonino
Departamento de Química, Facultad de Ciencias Exactas, Universidad Nacional de La Plata, Calle 115 y 47, Casilla de Correo 962, 1900 La Plata, República Argentina

(Received 22 April 1988; revised manuscript received 15 September 1988)

The optical parameters (namely, the complex dielectric tensor and refractive indexes) of sodium nitroprusside dihydrate (SNP), $Na_2[Fe(CN)_5NO]\cdot 2H_2O$ (orthorhombic, space group D_{2h}^{12}) in the infrared (ir) region 1550–2250 cm^{-1}, which includes the fundamental bands of the strongly polar NO stretching mode, are determined. For this purpose, transverse-electric (TE) reflectance data on the (100) and (010) faces of SNP in the range 250–4000 cm^{-1} were analyzed by the Kramers-Kronig (KK) dispersive method. The values obtained for the optical parameters were employed to get the wave numbers of transverse ($\bar{\nu}_{TO}$) and longitudinal ($\bar{\nu}_{LO}$) ir-active optic NO stretching modes of symmetry species B_{3u} (polarized along the **a** axis) and B_{2u} (polarized along **b**). It is shown that obtaining sharp peaks for accurate frequency measurements of the strong TO NO modes by transmission spectroscopy would require impossibly thin crystal films (of thicknesses of a few tenths of a micrometer), much smaller than the practical limit (a few tens of micrometers). Hence, our room-temperature values for $\bar{\nu}_{TO}$ of 1944 cm^{-1} (B_{3u} mode) and 1942 cm^{-1} (B_{2u} mode) should be considered more reliable than the corresponding transmission values reported in the literature. The KK dielectric tensor was also employed to compute the transverse-magnetic (TM), off-axis transmittance spectra of (100) and (010) SNP plates in the NO stretching region. These calculations are in good agreement with spectroscopic data and exhibit sharp peaks at 1964 and 1953 cm^{-1} due to the coupling of B_{3u} and B_{2u} LO modes, respectively, with the ir radiation. Our results show that strongly absorbing LO modes polarized perpendicularly to the plate can be easily identified through the variation of their band intensities with the incident angle of the ir beam and that their frequency can be accurately measured in relatively thick samples. The calculated TM-polarized, off-axis reflectance spectrum from the (010) face of thick SNP crystals for $\mathbf{E}\|ab$ is in reasonable agreement with experimental results and affords the interpretation of the observed bimodal spectral features in the NO stretching region as being due to a superposition of a reststrahlen band associated with the in-plane polarized TO mode and a band due to the reflection from the LO mode polarized perpendicularly to the crystal face.

I. INTRODUCTION

Orthorhombic sodium nitroprusside dihydrate (SNP), $Na_2[Fe(CN)_5NO]\cdot 2H_2O$, occupies a pivotal position in chemical, physical, and theoretical studies on the nitroprusside anion, $[Fe(CN)_5NO]^{2-}$. The first structural determination of this ion was carried out in SNP employing x-ray diffraction techniques.[1] The determined molecular architecture of this metal nitrosyl complex served as a basis for a fundamental work on SCCC-MO calculations of its electronic structure[2] and also for normal coordinates analysis of its vibrational behavior.[3–5] The infrared (ir) and Mössbauer spectra of SNP provide useful standards referred to in spectroscopic work.[6,7] Recently, interest in SNP has renewed because of the discovery of a long-living electronic metastable state of the anion produced by laser irradiation at low temperature.[8–11] This metastable state, which is supposed to arise from the $2b_2(d_{xy})\rightarrow 7e(\pi^*NO)$ electronic transition corresponding to the undistorted anion,[8] can also be produced in the barium salt $Ba[Fe(CN)_5NO]\cdot 3H_2O$ (BNP).[12] In this connection, SNP (and by extension BNP also) is considered as a potential optical-storage material.[13]

The spectroscopic properties of SNP in the visible and near-ultraviolet spectral regions have been dealt with in Ref. 2.

The vibrational behavior of SNP has been the subject of several studies by ir and Raman spectroscopic techniques.[14–19] There seems to be, however, no readily available study on the ir optical properties of the compound. To provide this information is one of the aims of the present work.

The substantial $d_\pi(\mathrm{Fe}) \rightarrow \pi^*(\mathrm{NO})$ back bonding existing in the $[Fe(CN)_5NO]^{2-}$ ion gives rise to a short Fe—N bond distance (1.64 Å) and is mainly responsible both for the electronic behavior in the ligand field region[2] and for the intense polarity associated with the NO stretching vibration of the complex.[20] Hence optic ir NO modes in SNP give place to intense, saturated bands in the absorption spectra even for the thinnest obtainable crystal plates (a few tens of micrometers).[18] This makes transmission measurements not useful for the precise determination of NO transverse-optical (TO) frequencies and reflection spectroscopy must be resorted to for this purpose. Also, the corresponding longitudinal-optical (LO) modes interact strongly with the ir radiation under certain conditions, giving place to sharp peaks substantially upshifted in frequency with respect to their TO counterparts in the transmission spectra. The accurate determination of TO and LO frequencies of SNP is another of the aims of this work. Incidentally, our results disclose previous misassignments in the SNP spectra reported in the literature.

We deal here with the ir optical properties and the revised vibrational structure of SNP in the spectral region between 1550 and 2250 cm^{-1} which includes the strong NO mode. The Kramers-Kronig dispersive analysis of the transverse-electric (TE) polarized reflectance data on principal faces of SNP will be employed to determine the optical parameters (namely, the dielectric tensor and refractive indexes) in the extended range 500–3800 cm^{-1}. These parameters will then be used to determine TO and LO frequencies of the ir-active optic modes. The determined dielectric tensor is employed to predict the profile and position of the NO bands for transverse-magnetic (TM) polarized, off-axis reflectance on the crystal (100) and (010) faces. Also, it is used together with theoretical expressions recently derived[21] to simulate on a computer the transmittance of SNP crystal plates that are practically impossible to obtain thin enough (less than 1 μm thick).

II. CRYSTALLOGRAPHIC AND SPECTROSCOPIC DATA OF $Na_2[Fe(CN)_5NO]\cdot 2H_2O$

The first crystal and molecular structure determination of SNP by photographic x-ray diffraction methods was reported in Ref. 1. A structure refinement of the compound employing more precise diffractometric data is reported in Ref. 22. SNP crystallizes in the orthorhombic space group $Pnnm$ (D_{2h}^{12}) with $a=6.198(2)$, $b=11.897(5)$, $c=15.557(5)$ Å, and $Z=4$. The complex anion exhibits a distorted octahedral configuration of ligands around Fe and lies on the crystallographic ab mirror plane. This plane bisects the angle formed by neighboring equatorial CN ligands. The FeNO group (which is practically linear) forms an angle of about 35° with the **a** axis.

The polarized ir transmittance spectra of SNP crystal plates parallel to the principal planes are shown in Refs. 14, 15, and 17–19. Raman spectra of the compound are reported in Refs. 16 and 18. A factor group analysis of the crystal vibrations leads to the following symmetry characterization and spectroscopic activities [ir and Raman (R)] of the optical modes: $A_g(R)$, $B_{1g}(R)$, $B_{2g}(R)$, $B_{3g}(R)$, B_{1u}(ir), B_{2u}(ir), B_{3u}(ir), and A_u(inactive). Because of the geometrical arrangement of the anions in SNP, the results for the optical NO stretching vibrations in the ir spectra are that the B_{1u} mode (polarized along **c**) should be absent, B_{2u} (polarized along **b**) should be very intense, and B_{3u} (polarized along **a**), should be stronger than B_{2u}. This is due to the larger projection of the intramolecular NO dipolar derivative ($\partial\boldsymbol{\mu}/\partial q$) along **a** than along **b**.

III. EXPERIMENT

Aqueous solutions of SNP were prepared from a recrystallized commercial product. Large single crystals (in the form of prisms elongated along the **a** axis) grew by spontaneous concentration of the solutions at room temperature and were crystallographically characterized as described in Ref. 23 for $Ba[Fe(CN)_5NO]\cdot 3H_2O$ (BNP). Plates were cut along principal planes with a thin diamond disk saw and the reflecting faces optically polished employing alcohol on cotton cloth stretched over a glass plate. The polarized specular reflection spectra were recorded at room temperature as reported for BNP (Ref. 23) and the digitalized data were sampled at 1-cm^{-1} intervals. Band positions were determined with an accuracy of 1 cm^{-1} for sharp bands and 2 cm^{-1} for broad ones.

IV. THEORY

For convenience, we will review here the electromagnetic basis for a quantitative description and interpretation of the reflectance and transmittance measurements in anisotropic absorbing crystals. For this purpose let us consider a face parallel to the principal xy plane of an orthorhombic (or more symmetric) crystal whose dielectric axes are labeled x, y, and z. Then, for monochromatic plane waves propagating along the xz plane and making an angle θ_i with the z axis, the fraction of the incident (i) amplitude for the s-polarized (TE) and p-polarized (TM) components reflected (r) from the xy crystal face are[24–26]

$$\tilde{r}_s = \frac{E_y^{(r)}}{E_y^{(i)}} = \frac{\cos\theta_i - (\tilde{\epsilon}_y - \sin^2\theta_i)^{1/2}}{\cos\theta_i + (\tilde{\epsilon}_y - \sin^2\theta_i)^{1/2}} , \tag{1a}$$

$$\tilde{r}_p = \frac{H_y^{(r)}}{H_y^{(i)}} = \frac{(\tilde{\epsilon}_x\tilde{\epsilon}_z)^{1/2}\cos\theta_i - (\tilde{\epsilon}_z - \sin^2\theta_i)^{1/2}}{(\tilde{\epsilon}_x\tilde{\epsilon}_z)^{1/2}\cos\theta_i + (\tilde{\epsilon}_z - \sin^2\theta_i)^{1/2}} , \tag{1b}$$

where E_y and H_y, respectively, stand for the y component of the electric and magnetic field vectors of the waves and $\tilde{\epsilon}_\alpha = \epsilon'_\alpha + i\epsilon''_\alpha$ ($\alpha = x,y,z$) are the complex principal values of the dielectric tensor $\tilde{\boldsymbol{\epsilon}}$. The phase spectrum $\theta(\bar{\nu})$ of the amplitude reflection coefficient $\tilde{r}_s(\bar{\nu})$ can be determined from a Kramers-Kronig dispersive analysis of the measured reflectance data $R_s = |\tilde{r}_s|^2$; the knowledge of $\theta(\bar{\nu})$ in turn affords the calculation of the optical parameters.[27]

From Eq. (1b), the TM reflectance $R_p = |\tilde{r}_p|^2$ can be expressed in the form

$$R_p = \left| \frac{\tilde{\epsilon}_x^{1/2}(\omega)\cos\theta_i - [1 - \sin^2\theta_i/\tilde{\epsilon}_z(\omega)]^{1/2}}{\tilde{\epsilon}_x^{1/2}(\omega)\cos\theta_i + [1 - \sin^2\theta_i/\tilde{\epsilon}_z(\omega)]^{1/2}} \right|^2 . \tag{2}$$

Equation (2) shows that in spectral regions where $\tilde{\epsilon}_z(\omega)$ presents resonances which are separated enough from the resonance of $\tilde{\epsilon}_x(\omega)$, two types of bands will appear in the reflection spectrum. One type includes the usual reststrahlen bands of x-polarized optic modes, and the other corresponds to the strong reflection which occurs at oblique incidence in the spectral range where $\tilde{\epsilon}_z(\omega)$ is small, that is, at about the longitudinal frequency of optic modes polarized along the z axis.[25,28]

The TE(s) and TM(p) transmittances through an orthorhombic crystal plate of thickness h bounded by smooth surfaces parallel to the xy principal plane are, respectively,[21]

$$T_s=\left|\cos(\delta\tilde{J}_y)-\frac{i}{2}\left[\frac{\tilde{J}_y}{\cos\theta_i}+\frac{\cos\theta_i}{\tilde{J}_y}\right]\sin(\delta\tilde{J}_y)\right|^{-2}, \tag{3a}$$

$$T_p=\left|\cos\left[\delta\left[\frac{\tilde{\epsilon}_x}{\tilde{\epsilon}_z}\right]^{1/2}\tilde{J}_z\right]-\frac{i}{2}\left[\frac{\tilde{J}_z}{\tilde{\epsilon}\cos\theta_i}+\frac{\tilde{\epsilon}\cos\theta_i}{\tilde{J}_z}\right]\sin\left[\delta\left[\frac{\tilde{\epsilon}_x}{\tilde{\epsilon}_z}\right]^{1/2}\tilde{J}_z\right]\right|^{-2}, \tag{3b}$$

where $\delta=\omega h/c$, $\tilde{J}_y=(\tilde{\epsilon}_y-\sin^2\theta_i)^{1/2}$, $\tilde{J}_z=(\tilde{\epsilon}_z-\sin^2\theta_i)^{1/2}$, and $\tilde{\epsilon}=(\tilde{\epsilon}_x\tilde{\epsilon}_z)^{1/2}$.

The s- and p-polarized transmittances of crystal plates bounded by rough surfaces are[21]

$$T_\mu=\frac{(1-R_\mu)^2e^{-\alpha\mu h}}{1-R_\mu^2e^{-2\alpha_\mu h}}\quad(\mu=s,p), \tag{4}$$

where

$$\alpha_s(\omega)=\frac{2\omega}{c}\,\mathrm{Im}\{[\tilde{\epsilon}_y(\omega)-\sin^2\theta_i]^{1/2}\}, \tag{5a}$$

$$\alpha_p(\omega)=\frac{2\omega}{c}\,\mathrm{Im}\left\{\left[\left[1-\frac{\sin^2\theta_i}{\tilde{\epsilon}_z(\omega)}\right]\tilde{\epsilon}_x(\omega)\right]^{1/2}\right\}, \tag{5b}$$

are the linear absorption coefficients for TE and TM waves, respectively. Equations (3a) and (4) for T_s describe the effect on the transmittance spectrum of crystal plates due to the usual absorption by TO modes. As discussed in detail in Ref. 21, Eqs. (3b) and (4) for T_p provide a quantitative account of LO peaks in the TM-polarized, off-axis transmittance spectra due to the coupling of ir radiation with LO modes polarized perpendicularly to the plate.

V. RESULTS AND DISCUSSION

Figure 1(a) shows the TE reflectance (R_s) spectrum on a (010) face of SNP (**E**$\|$**a**), at an angle of incidence $\theta_i=15°$, in the spectral region between 250 and 4000 cm^{-1}. The reststrahlen bands at about 650, 1600, 1950, 2150, and 3600 cm^{-1} are due to FeN stretching, H_2O bendings, and NO, CN, and H_2O stretching modes of B_{3u} symmetry, respectively. The peak at about 420 cm^{-1} and the overlapping broad feature in this spectral region can be assigned to FeC stretchings, FeCN deformations, and water librations.[18] Figure 1(b) depicts the TE reflectance data from a (100) face of SNP (**E**$\|$**b**) corresponding to B_{2u} optic modes.

Figure 2 shows the real part $\epsilon_x'(\bar{\nu})$ of $\tilde{\epsilon}(\bar{\nu})$ along the **a** axis of SNP, in the spectral range 1550–2250 cm^{-1}, obtained from Kramers-Kronig analysis of the reflectance data in Fig. 1(a).[29] A similar curve is obtained for $\epsilon_y'(\bar{\nu})$ by analyzing the data of Fig. 1(b). Figures 3(a) and 3(b) show the corresponding imaginary parts $\epsilon_x''(\bar{\nu})$ and $\epsilon_y''(\bar{\nu})$ along with plots of $-\mathrm{Im}(1/\tilde{\epsilon}_x)$ and $-\mathrm{Im}(1/\tilde{\epsilon}_y)$. The relatively small negative nonphysical values of these functions at about 1936 cm^{-1} are due to small negative values taken by the Kramers-Kronig phase angle θ_α ($\alpha=x,y$) in the same spectral region. This is due to experimental errors in the reflectance data and errors in the extrapolation of these data to the low- and high-wave-number re-

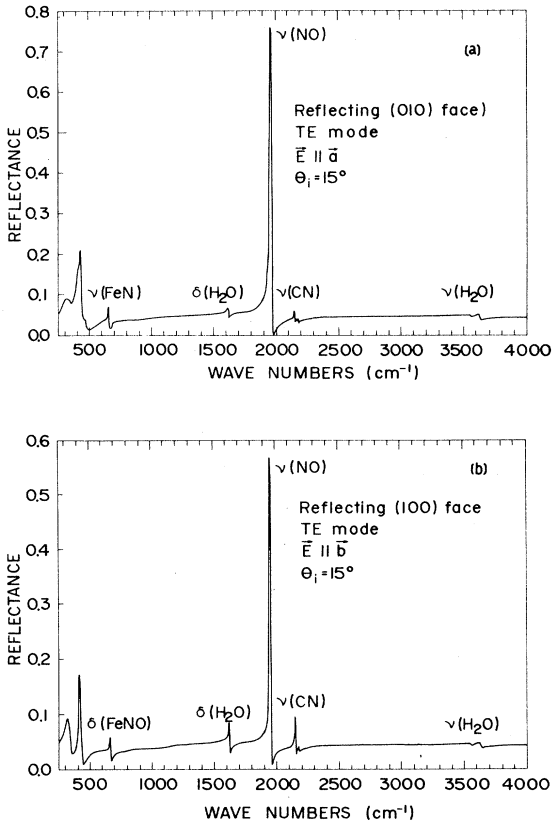

FIG. 1. Experimental transverse-electric (TE) infrared (ir) reflectance spectra from principal faces of $Na_2[Fe(CN)_5NO]\cdot2H_2O$ (SNP) at 15° incidence in the 250–4000 cm^{-1} spectral range. (a) (010) face, **E**$\|$**a**; (b) (100) face, **E**$\|$**b**.

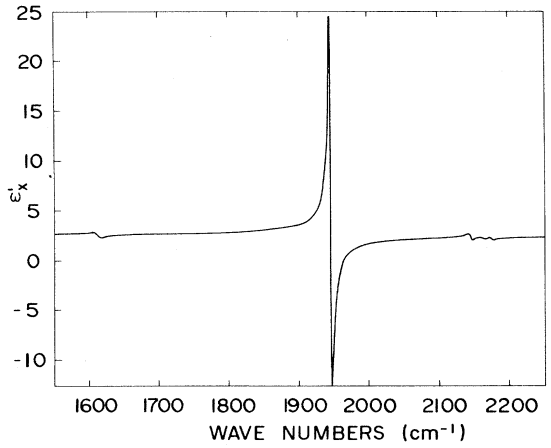

FIG. 2. Real part ϵ' of the dielectric permeability of SNP along **a** in the 1550–2250 cm^{-1} region.

gions of the spectra. A Kramers-Kronig calculation carried out in the extended range 500–3800 cm^{-1} shows no other nonphysical θ values. The peaks in ϵ''_x and ϵ''_y correspond to TO resonances of B_{3u} and B_{2u} modes, respectively, while the maxima of $-\mathrm{Im}(1/\tilde{\epsilon}_x)$ and $-\mathrm{Im}(1/\tilde{\epsilon}_y)$ occur at the wave number of the associated LO modes. The relatively large LO-TO splittings of the NO stretching vibrations (20 and 11 cm^{-1} for B_{2u} and B_{2u} modes, respectively) are due to the strong polarity of this vibration.[20,23,30,31] Calculated TO and LO wave numbers for the B_{3u} and B_{2u} resonances of Fig. 3 are collected in Table I, where they are compared with experimental data taken from Refs. 17 and 18. For the sake of completeness, this table also includes calculated and observed band positions for SNP in the low- and high-wave-number regions of the ir spectrum. Good agreement is noted between observed and calculated TO wave numbers for the less intense modes (which correspond to small LO-TO splittings). For these modes, transmission measurements through single crystal plates of realistic thickness (a few tens of micrometers) provide more intense and sharper peaks, and hence better resolution than the spectra derived from external reflectance data. The advantages of this technique over tranmission spectroscopy arise in connection with very strong absorptions. In particular, the obtaining of sharp peaks at the B_{3u} and B_{2u} NO resonances with minimum transmittance $T_s \sim 1/e$ and a full width at peak half height $\Delta\bar{\nu}_{1/2} \sim 9$ cm^{-1} would require impossibly thin samples of about 0.1 and 0.15 μm in thickness, respectively (see below). In fact, the room-temperature polarized ir transmittance spectra of a (001) SNP crystal plate of about 10 μm in thickness exhibit broad, saturated B_{3u} and B_{2u} bands centered at about 1945 and 1937 cm^{-1} with $\Delta\bar{\nu}_{1/2}$ widths of about 60 and 40 cm^{-1}, respectively.[18] This explains the discrepancy between the literature values included in Table I for the TO frequency of the optic NO stretching mode B_{2u} and the value 1942 cm^{-1} derived from reflectance data, which henceforth should be considered as a more precise determination of $\bar{\nu}_{\mathrm{TO}}$ for this mode. The coincidence of the three $\bar{\nu}_{\mathrm{TO}}$ values reported in Table I for the B_{3u} mode should therefore be considered as fortuitous.

The refractive index $[n_x(\bar{\nu})]$ and extinction coefficient $[k_x(\bar{\nu})]$ of SNP for TE waves polarized along **a** in the range 1550–2250 cm^{-1} are plotted in Fig. 4. Similar curves are obtained for the real $[n_y(\bar{\nu})]$ and imaginary $[k_y(\bar{\nu})]$ parts of the complex refractive index along **b**. At the high-wave-number edge of the ir spectral region considered in this work (4000 cm^{-1}), which is far beyond the fundamental transition of highest wave number of ir-active SNP crystal vibrations, the calculated refractive indexes n_x and n_y attain constant values equal to 1.55 and 1.53, respectively. These values are consistent with the values measured in the visible spectral region (see the last of Refs. 8). The peak k_μ ($\mu=x,y$) values at NO resonances are about 4.2 (B_{3u} mode) and 2.8 (B_{2u} mode). These values lead to maxima in the corresponding linear absorption coefficients $\alpha_\mu=4\pi\bar{\nu}_\mu k_\mu$ (TO, $\mu=x,y$) of about 1×10^5 and 0.7×10^5 cm^{-1} at the B_{3u} and B_{2u} res-

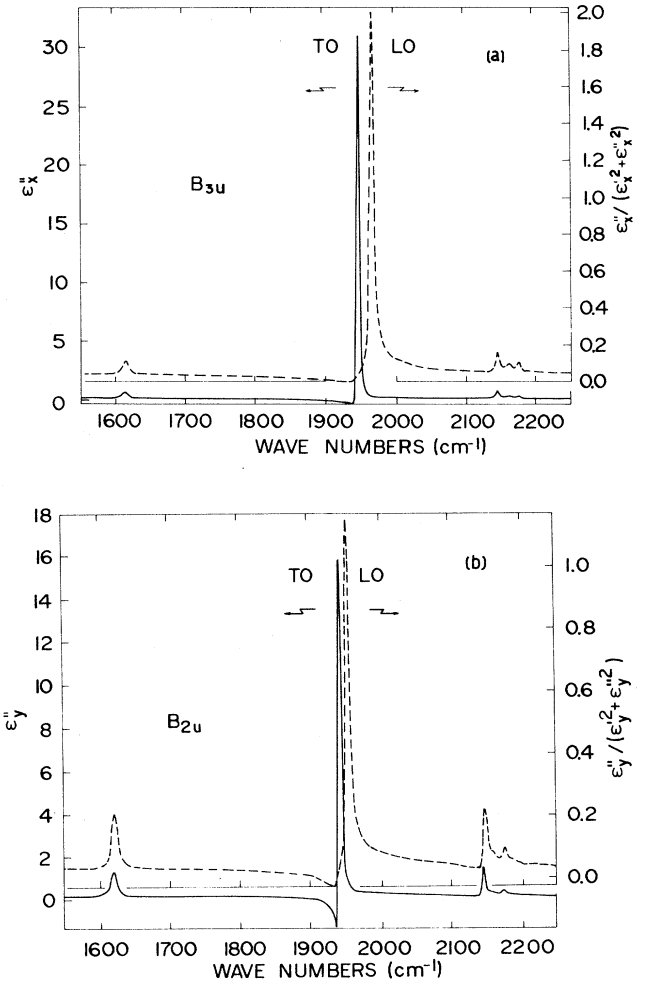

FIG. 3. Solid lines, imaginary parts ϵ'' of the dielectric permeability of SNP along **a** (a) and along **b** (b). Dashed lines, plots of $-\mathrm{Im}(1/\tilde{\epsilon}_\alpha)=\epsilon''_\alpha/(\epsilon'^2_\alpha+\epsilon''^2_\alpha)$ ($\alpha=x,y$).

TABLE I. Calculated TO and LO wave numbers for B_{3u} and B_{2u} resonances of SNP in the 500–3800 cm^{-1} spectral range and ir data taken from Refs. 17 and 18.

This work		Ref. 17		Ref. 18		
$\bar{\nu}_{TO}$	$\bar{\nu}_{LO}$	$\bar{\nu}_{TO}$	$\bar{\nu}_{LO}$	$\bar{\nu}_{TO}$	$\bar{\nu}_{LO}$	Assignment
			(a) B_{3u} modes			
651	653	654		652		ν(FeN)
1613	1614	1618		1611		$\delta(H_2O)$
1944	1964	1945	1963	1945	1965[a]	ν(NO)
2145	2145	2143		2144		ν(CN)
2162	2162	2162		2161		ν(CN)
2174	2175	2173		2173		ν(CN)
3546	3549	3550		3550		$\nu(H_2O)$
3620	3621	3630		3625		$\nu(H_2O)$
			(b) B_{2u} modes			
662	664	665		661		δ(FeNO)
1619	1621	1614		1616		$\delta(H_2O)$
1942	1953	1945	1963	1937	1945[b]	ν(NO)
2145	2148	2143		2144		ν(CN)
2160sh[c]	2160sh	2162		2161		ν(CN)
2174	2176	2173		2173		ν(CN)
3548	3550	3550		3550		$\nu(H_2O)$
3627	3630	3630		3625		$\nu(H_2O)$

[a]Assigned in Ref. 18 as an additive combination band (see text).
[b]Assigned in Ref. 18 as a B_{1u} mode.
[c]sh: shoulder.

onances, which determine the optimal SNP sample thicknesses of about 0.1 and 0.15 μm, respectively, mentioned above.

Figure 5 shows the predicted polarized ir transmittance (T_s) spectra of two very thin SNP crystal plates (0.1 μm thick) bounded by smooth surfaces parallel to (010) and (100) planes for normal incidence of an ir beam polarized along **a** (solid line) or **b** (dashed line), respectively. The calculations were performed employing in Eq. (3a) the Kramers-Kronig dielectric permeabilities $\tilde{\epsilon}_\alpha = \epsilon'_\alpha + i\epsilon''_\alpha$ ($\alpha = x,y$). As expected from the limiting form of Eq. (3a) for the transmittance of very thin plates,[21,23] the sharp transmittance minima in Fig. 5 coincide in spectral positions with the corresponding peaks of ϵ''_x and ϵ''_y in Fig. 3. The transmission spectra computed under the same conditions as for the spectra of Fig. 5 but now assuming a sample thickness of 1 μm are shown in Fig. 6. From this figure it can be appreciated that even

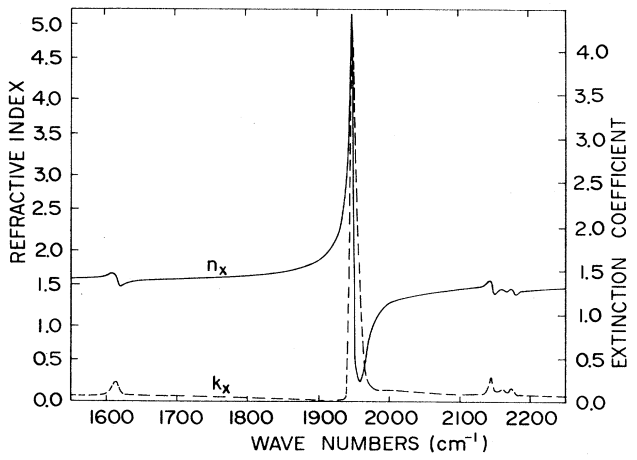

FIG. 4. Solid and dashed lines, respectively, are the refractive $n(\bar{\nu})$ and extinction coefficient $k(\bar{\nu})$ indexes of SNP along **a**.

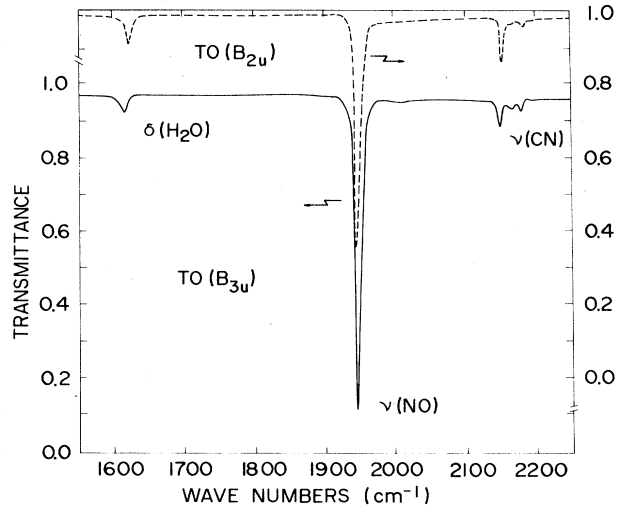

FIG. 5. TE transmittance (T_s) spectra of very thin crystal plates (0.1 μm thick) of SNP bounded by smooth surfaces for normal incidence of the ir beam in the spectral range 1550–2250 cm^{-1}, calculated with Eq. (3a). Solid line, T_s of a (010) plate for **E**||**a**; dashed line, T_s of a (100) plate for **E**||**b**.

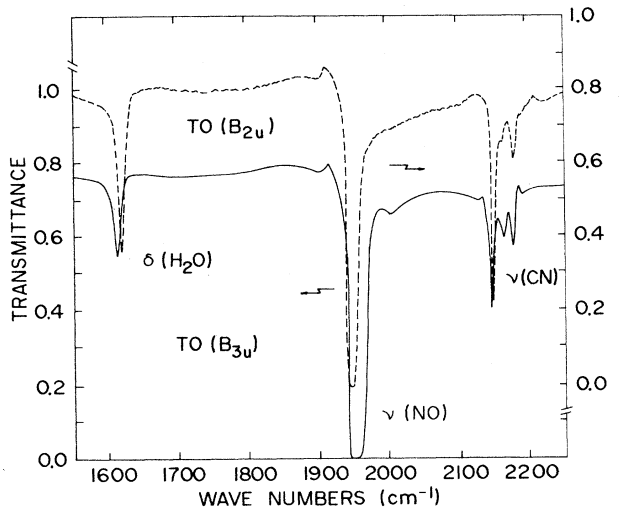

FIG. 6. Same conditions as for Fig. 5, but now plate thicknesses are 1 μm.

for thicknesses of about ten times smaller than the practical limit, optic NO stretching resonances B_{3u} and B_{2u} would still appear as broad saturated bands of about 25 and 17 cm^{-1} width at half height, respectively.

Figure 7 shows the computed TM transmittances (T_p) of a SNP (100) crystal plate with rough surfaces in the spectral range 1850–2050 cm^{-1} which includes the strong NO stretching modes. The calculations were carried out with Eqs. (4) and (5b) for T_p assuming that the incident ir beam lies on an *ab* plane and makes angles of 15° (solid line) and 30° (dashed line) with the **a** axis. In Fig. 7 we may notice that on the high-wave-number side of the broad TO (B_{2u}) band there appears a sharp peak at 1964 cm^{-1} whose intensity increases with the angle of incidence. From an analysis of Eqs. (4) and (5b) for T_p, we conclude that this peak should be assigned to the B_{3u} longitudinal NO stretching optic mode polarized perpendicularly to the plate which gives place to a peak at the same spectral position in the $-\mathrm{Im}(1/\bar{\epsilon}_x)$ plot of Fig. 3(a). This band was already observed at 1965 cm^{-1} in the low-temperature (80 K) spectra of SNP (Ref. 18) but misassigned as an additive combination band of NO stretching and librational vibrations of the nitroprusside ion. The same band observed at 1963 cm^{-1} in the ir spectra of SNP at 300 K was correctly attributed to a longitudinal-optic mode associated with the NO stretch, and its appearance was explained as due to the convergence of the incident ir beam.[17] A complete characterization regarding the factor group symmetries and polarizations of the two LO modes derived from the NO stretching vibrations was not provided, however.[17] As expected, the LO peak due to the optic NO B_{3u} mode can also be

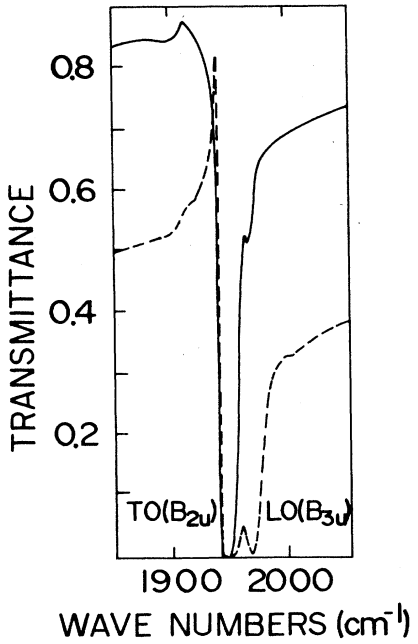

FIG. 7. Computed transverse-magnetic (TM) transmittance (T_p) spectra in the NO stretching region of a thin SNP crystal plate (1 μm thick) with rough surfaces parallel to (100), for an incident ir beam lying on the *ab* plane and making angles of 15° (solid line) and 30° (dashed line) with **a**. The calculations were performed employing, in Eqs. (4) and (5b) for T_p, the Kramers-Kronig dielectric permeabilities $\bar{\epsilon}_\alpha = \epsilon'_\alpha + i\epsilon''_\alpha$ ($\alpha = x,y$).

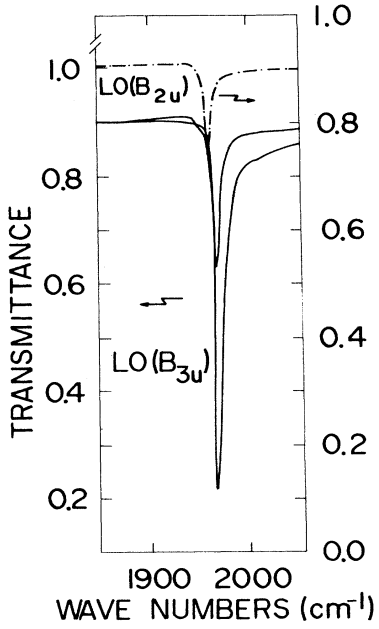

FIG. 8. Computed TM transmittance (T_p) spectra of SNP crystal plates (12 μm thick) bounded by rough surfaces, in the NO stretching region. The spectra in solid lines correspond to T_p of a (100) plate for $\mathbf{E} \| ac$ and angles of incidence $\theta_i = 10°$ (lower curve) and $\theta_i = 5°$ (middle curve). The spectrum in the upper part of the figure corresponds to T_p of a (010) plate for $\mathbf{E} \| bc$ and $\theta_i = 5°$. The calculations were carried out assuming in Eqs. (4) and (5b) a constant ϵ_z value (2.46) in the NO stretching region.

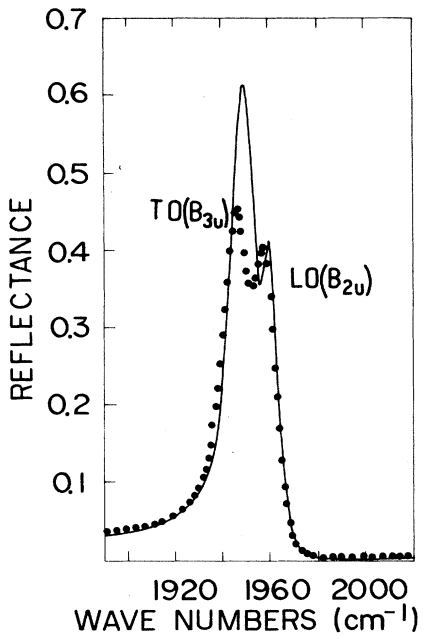

FIG. 9. Experimental (dots) and calculated (lines) TM reflectance (R_p) spectra on a (010) SNP face in the NO stretching region for an incident ir beam lying on the *ab* plane and making an angle of 45° with **b**.

seen in the TM, off-axis transmittance spectra of relatively thick (100) SNP plates when the plane of incidence is *ac*, but now with the advantage that no overlapping transverse-optic NO band is present due to the orientation of the nitroprusside ions in the crystal. This is shown in the calculated spectra of Fig. 8 (solid lines) and confirmed in the observed polarized transmission spectra of (100) plates of SNP reported in Refs. 17 and 18. Figure 8 also includes the computed TM transmittance of a (010) plate 12 μm thick for an incident ir beam lying on the *bc* plane and making an angle $\theta_i = 5°$ with the **b** axis. The sharp peak at 1953 cm^{-1} is due to the longitudinal-optic mode of B_{2u} symmetry that gives rise to a peak at about the same wave number in the spectrum of $-\mathrm{Im}(1/\tilde{\epsilon}_y)$ in Fig. 3(b). This peak was also observed in Ref. 18 (at 1945 cm^{-1}) but misassigned as a B_{1u} TO mode.

In Fig. 9 the observed TM reflectance spectrum (R_p) from a (010) face of SNP in the range 1890–2020 cm^{-1} for an ir beam lying on the *ab* plane and making an angle of 45° with the **b** axis is compared with the spectrum calculated through Eq. (2). As described for the general case in Sec. IV, the spectra can be interpreted as a superposition of a reststrahlen band located at about 1950 cm^{-1} due to the B_{3u} TO mode (polarized along **a**), and a band at about 1960 cm^{-1} due to reflection from the B_{2u} LO mode (polarized along **b**).

ACKNOWLEDGMENTS

We thank Dr. S. R. González for her assistance during part of the experiments. This work was supported by the following institutions: Consejo Nacional de Investigaciones Científicas y Técnicas (CONICET), Comisión de Investigaciones Científicas de la Provincia de Buenos Aires, República Argentina, and Financiadora de Estudos e Projetos and Fundacão de Amparo a Pesquisa do Estado de São Paulo, Brazil. Support from the exchange program between CONICET and Conselho Nacional de Desenvolvimento Científico e Tecnológico (Brazil) is also gratefully acknowledged.

[1]P. T. Manoharan and W. C. Hamilton, Inorg. Chem. **2**, 1043 (1963).
[2]P. T. Manoharan and H. B. Gray, J. Am. Chem. Soc. **87**, 3340 (1965).
[3]G. Paliani, A. Poletti, and A. Santucci, J. Mol. Struct. **8**, 63 (1971).
[4]B. B. Kedzia, B. Jezowska-Trzebiatowska, and J. Ziólkowski, Bull. Acad. Pol. Ser. Sci. Chim. **20**, 237 (1972).
[5]B. N. Cyvin, S. J. Cyvin, A. Zabokrzycka, and B. B. Kedzia, Spectrosc. Lett. **16** 249 (1983).
[6]C. O. Della Védova, J. L. Lesk, E. L. Varetti, P. J. Aymonino, O. E. Piro, B. E. Rivero, and E. E. Castellano, J. Mol. Struct. **70**, 241 (1981).
[7]W. L. Gettys and J. G. Stevens, in *Handbook of Spectroscopy*, edited by J. W. Robinson (Chemical Rubber Company, Boca Raton, FL, 1974), Vol. III, p. 496.
[8]U. Hauser, V. Oestreich, and H. D. Rohrweck, Z. Phys. A **280**, 17 (1977); **280**, 125 (1977); **284**, 9 (1978).
[9]Th. Woike, W. Krasser, P. S. Bechthold, and S. Haussühl, Solid State Commun. **45**, 499 (1983); **45**, 503 (1983); J. Mol. Struct. **114**, 57 (1984).
[10]W. Krasser, Th. Woike, S. Haussühl, J. Kuhl, and A. Breitschwerd, J. Raman Spectrosc. **17**, 83 (1986).
[11]J. A. Güida, O. E. Piro, and P. J. Aymonino, Solid State Commun. **57**, 175 (1986).
[12]J. A. Güida, O. E. Piro, and P. J. Aymonino, Solid State Commun. **66**, 1007 (1988).
[13]Th. Woike, W. Krasser, and P. Bechthold, Phys. Rev. Lett. **53**, 1767 (1984).
[14]A. Sabatini, Inorg. Chem. **6**, 1756 (1967).
[15]L. Tosi, C. R. Acad. Sci. **265**, 1020 (1967).
[16]R. K. Khanna, C. W. Brown, and L. H. Jones, Inorg. Chem. **8**, 2195 (1969).
[17]J. Bates and R. K. Khanna, Inorg. Chem. **9**, 1376 (1970).
[18]L. Tosi, Spectrochim. Acta Part A **26**, 1675 (1970).
[19]L. Tosi, Spectrochim. Acta Part A **29**, 353 (1973).
[20]B. Folkesson, Acta Chem. Scand., Ser. A **28**, 491 (1974).
[21]O. E. Piro, Phys. Rev. B **36**, 3427 (1987).
[22]F. Bottomley and P. S. White, Acta Crystallogr. Sect. B **35**, 2193 (1979).
[23]O. E. Piro, S. R. González, P. J. Aymonino, and E. E. Castellano, Phys. Rev. B **36**, 3125 (1987).
[24]L. P. Mosteller, Jr. and F. Wooten, J. Opt. Soc. Am. **58**, 511 (1968).
[25]J. C. Decius and R. M. Hexter, *Molecular Vibrations in Crystals* (McGraw-Hill, New York, 1977), pp. 183–193.
[26]The tilde in Eq. (1) and in other mathematical expressions throughout the text emphasizes quantities which are complex

numbers.
[27]F. Stern, in *Solid State Physics,* edited by F. Seitz and D. Turnbull (Academic, New York, 1963), Vol. 15, pp. 327–342.
[28]J. C. Decius, R. Frech, and P. Bruesch, J. Chem. Phys. **58**, 4056 (1973).
[29]In the Kramers-Kronig calculation, it was assumed a constant value for R_s beyond 4000 cm^{-1}; the low-wave-number region below 250 cm^{-1}, out of reach of our equipment, has not been considered.
[30]S. R. González, P. J. Aymonino, and O. E. Piro, J. Chem. Phys. **81**, 625 (1984).
[31]S. R. González, O. E. Piro, P. J. Aymonino, and E. E. Castellano, Phys. Rev. B **33**, 5818 (1986).